Hemodynamic Physiology in Aortic Arch and Trigger Factors of Atherosclerosis

F. I. Todua and M. V. Beraya

Translated from *Byulleten' Eksperimental'noi Biologii i Meditsiny*, Vol. 140, No. 12, pp. 614-617, December, 2005
Original article submitted March 22, 2005

Magnetic resonance angiography showed that blood flow in the aortic arch during protodiastole is separated into the opposite flows, which are temporarily arrested at the certain sites creating the flat front of the flow. The protodiastolic antegrade peak acceleration 6-fold surpasses the systolic one. Due to adhesion, the high gradient pressure forces can damage the vascular wall.

Key Words: *magnetic resonance angiography; atherosclerosis; protodiastole; flat flow; shear stress*

Generalized or chronic inflammation is one of the pathogenic mechanisms of atherosclerosis. The problem of etiological factors provoking atherosclerosis remains controversial.

Atherosclerotic damages to vessels appear in certain sites of the circulatory system. They are caused by low level of shear stress, appearance of re-circulatory blood flow zones, and prolongation of cell-cell interactions [5, 7-9]. It is considered that arterial thickening promotes restoration of shear stress and tensile stress [6-10].

Our aim was to study the peculiarities of blood flow in the aortic arch using magnetic resonance angiography (MRA).

MATERIALS AND METHODS

The hemodynamic indices in the ascending and descending part of the aortic arch were examined in 14 healthy men aging 27-35 years (HR 70±5 min^{-1}, blood pressure 125/80±10 mm Hg). Complex clinical examination and biochemical tests of the blood (lipid status, ECG, trans-thoracic echocardiography, and MRA performed with a Siemens-Sonata-Cardio 1.5T apparatus tuned to f12D, repetition time 24.6 msec, echo-time 1.5 msec, visual field 348×360, section 6 mm; repetition time 47 msec, echo-time 2.7 msec, examination time 19.30, visual field 292×360, and section 6 mm) were performed in all examinees.

MRA images were triggered by ECG during breath holding. The examined parameters were the mean and peak velocity as well as the mean and true flow. The measurements were carried out in 11 different levels in the opposite aortic walls (from Valsalva sinuses to the distal part of the thoracic aorta) on the sites with the area of about 0.7 cm^2.

RESULTS

It is an experimental problem to obtain precise hemodynamic data in large arteries by MRA, so we used aorta as the object with characteristic flow areas and pronounced shear stress (Table 1). Due to circulatory movement of the blood and the existence of additional centrifugal force, blood flows with different velocities at the opposite aortic walls are formed [2,4] (Fig. 1, 2). In the entrance of the aorta, the systolic velocity is grater at the external side. Within the aortic arch, the systolic velocity increased towards the internal side (Fig. 2). In the circular movement, the velocity vector was directed

Department of Magnetic Resonance Tomography, Institute of Medical Radiology, Tbilisi. ***Address for correspondence:*** mberaia@hotmail.com. M. V. Beraya

0007-4888/05/1406-0664

TABLE 1. Hemodynamic Indices in Aortic Arch (*M*±*m*, cm/sec)

Index, aortic wall		Entrance into arising aorta	Aorta origin	Central part of the aorta	Isthmus	Entrance into thoracic aorta	Central part of the thoracic aorta
Velocity							
peak systolic	external side	84.5±2.1	46.7±1.5	47.8±0.4	60.1±1.2	68.5±1.9	58.4±1.3
	internal side	71.7±1.7	56.9±2.1	59.3±1.8	74.7±2.5	68.2±1.5	54.9±1.3
protodiastolic	external side	22.3±0.7	-44.8±1.0	-55.3±0.7	—	-12.7±0.3	-18.7±0.7
	internal side	-48.5±0.5	-13.3±0.7	-13.3±0.3	-10.4±0.6	-127.6±10.3	-122.4±15.4
retrograde	external side				142.6±10.2		
antegrade	external side	49.5±1.5	25.3±1.5	30.1±0.4	128.7±9.9	17.5±0.5	
	internal side	20.3±0.3	15.5±0.6	-10.1±0.2	20.5±0.5	133.8±12.7	40.7±0.7
Systolic acceleration	external side	563.7±11.2	375.8±8.4	315.4±7.2	402.4±10.1	456.3±9.3	389.2±9.2
	internal side	476.5±9.3	308.7±9.1	375.8±8.9	496.6±8.9	456.3±7.4	389.2±9.4
protodiastolic	external side	-467.2±9.4	-375.8±7.8	-953.2±17.3	—	-397.2±0	-389.2±8.5
	internal side	-1112.1±26.8	-308.7±7.8	-392.5±7.2	-362.4±7.8	-1763.8±37.5	-2309.8±49.9
retrograde	external side				1887.8±41.5		
antegrade	external side		127.9±12.3	1666.6±35.4	2523.3±47.8	576.8±9.3	
	internal side	518.8±10.3	53.6±1.1		52.2±0.7	3611.1±77.8	2253.5±47.8
Blood flow velocity in the flat flow region in protodiastole		19.0±1.3	0±0.2	5.3±1.2	0±0.1	10.7±1.8	18.6±2.2

tangentially to the trajectory and distally to the aortic isthmus, where the circular movement was transformed into the linear one. A large systolic velocity was observed at the external side near the origin of the thoracic aorta (Table 1).

In the isthmus region, MRA data showed that the blood flow separated on millisecond 185. On millisecond 203, these flows were oppositely directed and oscillated with different periods. On millisecond 300, the flow was delayed (Fig. 1), and the periods were equalized when the velocity zeroed. During the following 0.3 msec, the blood velocity increased from 0 to 1 cm/sec. At the external side, the protodiastolic acceleration of the blood flow 6-fold surpassed the systolic one.

Atheromatous degeneration of vessels can result from predisposition of some vascular regions to the development of atherosclerotic process. Otherwise, it can be triggered by various hemodynamic influences on the arterial walls.

The forces affecting the arterial walls are the near-wall shear stress with tangentially directed vector (1.5 N/m^2 on average) and transmural pressure (tensile stress, 150 N/m^2 on average) directed normally to the aortic wall. When the near-wall shear stress exceeds 40 N/m^2, it can damage the endothelial cells [2].

MRA showed that in zones with low systolic shear stress, the protodiastolic shear stress is considerably higher than in zones with high systolic shear stress. For example, at the external side of the aorta, systolic shear stress (τ) attains 3.07-3.83 N/m^2, the protodiastolic shear stress being 7.04-18.18 N/m^2.

Shear stress was calculated by the formula

$$\tau=2\alpha\mu v/d \quad (1)$$

where α is Womersley frequency number, μ is apparent viscosity, v is flow velocity, and d is flow diameter.

The movement of each element of the fluid was determined by the following equation:

$$\text{mass}\times\text{acceleration}=\text{viscous force (shear stress)}+\text{massive force (weight)}+\text{+pressure gradient} \quad (2)$$

In this equation, the weight can be neglected because of horizontal position of the vessel. In this case, acceleration is proportional to shear stress and pressure gradient.

The blood flow is pulsing. In the aortic arch, the external part of the flow (with greater curvature) is separated during protodiastole. It changes the velocity and moves in the retrograde direction. After closure of the aortic valves, the blood moves again in the antegrade direction. In zones with low systolic velocity, the protodiastolic acceleration 6-fold surpasses the systolic one.

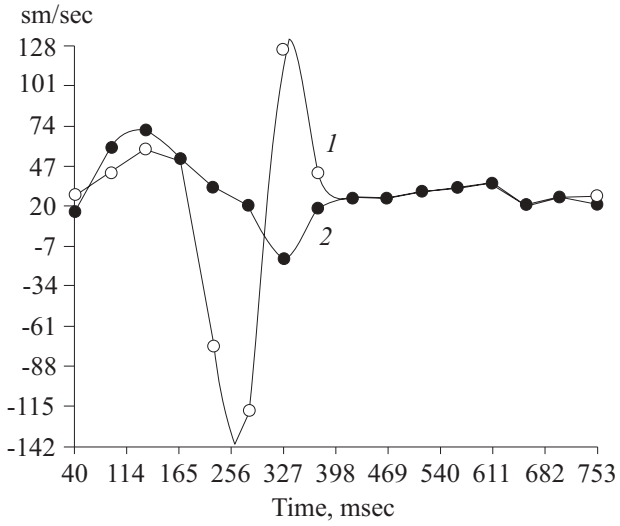

Fig. 1. Peak velocity in zones on the external (*1*) and internal (*2*) side of the aortic isthmus.

During conversion of protodiastolic retrograde flow into the antegrade flow, an instantaneous local delay of aortic blood flow occurs synchronously with the oppositely directed flow. At this moment, the flow profile in this zone is flat, the boundary layer is absent, and all elements of the blood flow move identically.

At zero (or peak) velocity, the gradient pressure is equal to the value reciprocal to the force of viscous resistance (shear stress or adhesion).

After the onset of the blood flow, the gradient force markedly decreases, although at the onset of protodiastolic antegrade flow, it significantly exceeds the value of 18.18 N/m^2 at the external side of the aortic arch.

At the start of movement of the blood elements, the tensile stress can be high. At this moment, the gradient pressure forces are counterbalanced by adhesion and inertia. During the initiating phase of motion and acceleration of the blood elements, the flow has no time to divide into the mutually sliding layers, so "sharpening" of the blood flow originates from the convexital surface of the layer.

At the start of movement, initially high transmural (tensile) pressure is uniformly spread in all directions, including the external adhesion fluid layer.

In zone with pronouncedly decreased velocity, high transmural pressure underlies attainment of limiting adhesion, which should be calculated starting from the surface strength of the blood. Manifestation of adhesion during initiation of the flow is caused by high apparent viscosity of the blood,

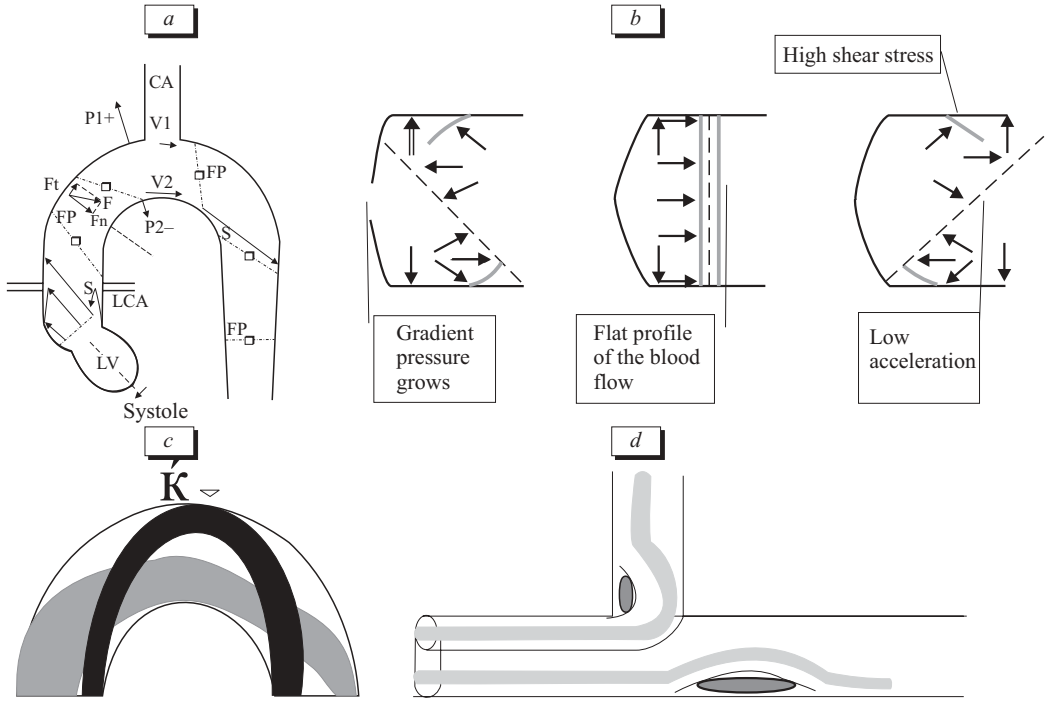

Fig. 2. Peculiarities of aortic blood flow. *a*) blood flow in the aortic arch: V1-V2, velocity, P1-P2, pressure at different walls of the vessel, Fn, Ft — normal and tangential pressure components, FP — front of the spreading wave, S — the places of separation of the boundary with reverse flow during systole, LV — left ventricle, LCA — left coronary artery, CA — carotid artery; *b*) formation of the flow with flat profile at high shear stress during protodiastole (the arrows show the direction of pressure force); *c*) separation of the blood flow during protodiastole into antegrade and retrograde flows (the arrow marks the critical site); *d*) peculiarities of the blood flow in zone of arterial branching. In *c*) and *d*) the retrograde flow is shown by black color.

which grows by more than 80 times at shear velocity below 0.1 sec^{-1} [2].

In this case, it is more correct to consider widening of convexital surface of the blood, rather than sliding of fluid layers.

At the external side of the aortic arch, the protodiastolic acceleration of the blood flow 6-fold surpasses the systolic one. At the onset of movement, the gradient pressure 6-fold surpasses the systolic pressure [3]. However, no lysis of erythrocytes occurs under these conditions, because the threshold shear stress for damage to erythrocytic membrane is 200-300 Nm^2.

During the retrograde phase of protodiastole, the opposite flows are characterized by different periods of oscillations resulting in complicated interference of the blood flow waves. Similar character of the blood flow takes place also at the arterial branching sites.

Accumulation of LDL cholesterol in the atherosclerotic plaque can be caused by the necessity to strength the stability of the plaque membrane. During atherosclerotic inflammation, the character of the near-wall flow and pressure forces change due to fibrosis and arterial calcinosis.

In vertebrates, the development of the aortic arch can be shaped by several factors. In this vessel, the retrograde blood flow promotes rapid closure of the aortic valves and filling of the left coronary artery, which lacks the systolic blood flow. During the circular movement of the blood, the pressure forces are greater at the external side of the blood vessel than at its internal side (the examples are aortic arch, cavernous sinus, and the clavicular artery). The large vessels arise from the external side of the arch and vascularize organs, which in birds and mammals can ascend higher than the horizontally located thoracic aorta (unilateral aorta and experimental atherosclerosis were observed only in these species) and therefore need additional pressure drive.

As the secondary activator of the blood flow, the aortic arch contributes into the due supply of the blood in all directions. In mammals, the vascular endothelium balances on the brink of tolerance to the gradient pressure forces, which promote damage to the walls of large arteries.

REFERENCES

1. S. A. Balezin, B. V. Erofeev, and Ya. I. Podobaev, *The Principles of Physical and Colloidal Chemistry* [in Russian], Moscow (1975).
2. C. Caro, T. Pedi, R. Schroter, and W. Seed, *Mechanics of Circulation* [Russian Translation], Moscow (1981).
3. M. V. Beraia and F. I. Todua, *Eur. Radiol.*, **12**, No. 11, 117-118 (2002).
4. Y. C. Fung, *Biomechanics, Circulation,* New York (1997).
5. D. N. Ku, D. P. Giddens, C. K. Zarins, and S. Glago, *Arteriosclerosis*, **5**, No. 3, 293-302 (1985).
6. B. L. Langille, *J. Cardiovasc. Pharmacol.*, **21**, Suppl. 1, S11-S17 (1993).
7. R. M. *Nerem, J. Biomech. Eng.*, **115**, No. 4B, 510-514 (1993).
8. R. Ross, *Nature*, **362**, 801-809 (1993).
9. C. K. Zarins, D. P. Giddens, B. K. Bharadvaj, *et al., Circ. Res.*, **53**, No. 4, 502-514 (1983).
10. C. K. Zarins, M. A. Zatina, D. P. Giddens, *et al., J. Vasc. Surg.*, **5**, 413-420 (1987).